Earth Reinforcement Practice, Ochiai, Hayashi & Otani (eds) © 1992 Balkema, Rotterdam. ISBN 90 5410 093 1

# Interaction between grid reinforcement and cohesive-frictional soil

D.T.Bergado, J.C.Chai & A.S.Balasubramaniam
*Asian Institute of Technology, Bangkok, Thailand*

ABSTRACT: Large scale direct shear and pullout tests have been conducted to investigate the interaction behavior between grid reinforcement and cohesive-frictional soil. The direct shear resistance between Tensar grids and cohesive-frictional soil such as weathered Bangkok clay is lower than the soil strength at peak strength condition, but higher than the soil strength at large displacement condition due to the mutual effects of the grid smooth plane surface and the apertures on the grids. An analytical method of determining the pullout force/pullout displacement curve is established based on linear elastic-perfect plastic skin friction model, hyperbolic pullout bearing resistance model, and load transfer mechanism developed for axially loaded pile by using the basic soil and grid reinforcement properties. Good agreement has been obtained between calculated values and test results. The method provides a useful tool for reinforced earth design.

## 1 INTRODUCTION

The mechanism governing soil/reinforcement interaction in a reinforced earth structure is concerned with mobilization of soil/reinforcement friction resistance, soil passive bearing resistance on reinforcement bearing members, and the bending movement in the reinforcement. Ignoring the reinforcement bending effect, the soil/reinforcement interaction mechanism can be simplified into two types, namely: soil sliding over the reinforcement or direct shear mechanism and pullout of the reinforcement from the soil or pullout mechanism. Direct shear and pullout tests are used to simulate these two different mechanisms, respectively. Direct shear test provides a local shear stress/shear displacement relationship, whereas pullout test integrates the variation in the shear stress and displacement along the reinforcement. Figure 1 shows a typical reinforced earth structure in a reinforced soil slope. Assuming that the dashed line in the figure is a potential failure surface, the reinforcement behind the potential failure surface, position A, will be subjected to pullout interaction mechanism. At the position B, the direct shear mechanism is likely to occur. The suitability of grid reinforcements for reinforcing the soil has been demonstrated by laboratory and field studies (Chang et al 1977; Peterson & Anderson 1980). Their potential use in cohesive-frictional soils is particularly attractive and has provided an incentive for research.

Large scale direct shear and pullout tests have been conducted to investigate the interaction mechanism between grid reinforcements and cohesive-frictional soils such as weathered Bangkok clay. The results are analyzed and presented in this paper. The relationship between direct shear or pullout resistance and relative displacement is also investigated.

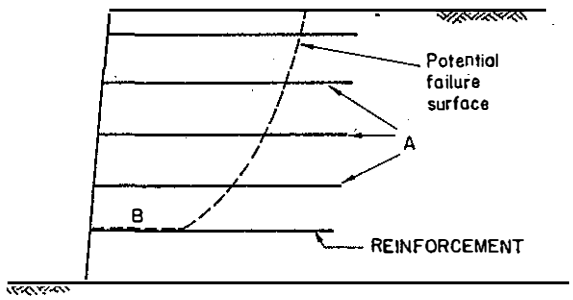


Fig. 1 Typical reinforced slope showing the soil/reinforcement interaction modes. A - pullout; B - direct shear

## 2 LABORATORY TEST PROGRAM

A total of 9 large scale direct shear and 60 pullout tests have been conducted by using weathered Bangkok clay as backfill material and welded wire steel grids and Tensar grids as reinforcements. The index properties of weathered Bangkok clay are listed in Table 1.

The pullout apparatus has been described in detail by Bergado et al (1992), which has inside dimension of 1.27 m in length by 0.76 m in width by 0.51 m in height (50x30x20 inches). The pullout force was applied by a 225 kN capacity electro-hydraulic controlled jack, and the normal pressure was applied by a pressurized air bag positioned between the soil and

**Table 1. Index properties of weathered Bangkok clay**

| | | |
|---|---|---|
| Specific gravity, G | | 2.67 |
| Plastic limit, $W_p$ (%) | | 21.0 |
| Liquid limit, $W_l$, (%) | | 45.0 |
| Plasticity index, $I_p$ | | 24.0 |
| Grain size | Sand, % | 17.4 |
| distribution | Silt, % | 24.4 |
| | Clay, % | 58.2 |
| United Classification system | | CL |
| Standard Proctor | Optimum water content,% | 23.0 |
| compaction | Maximum dry density, kN/m$^3$ | 16.0 |

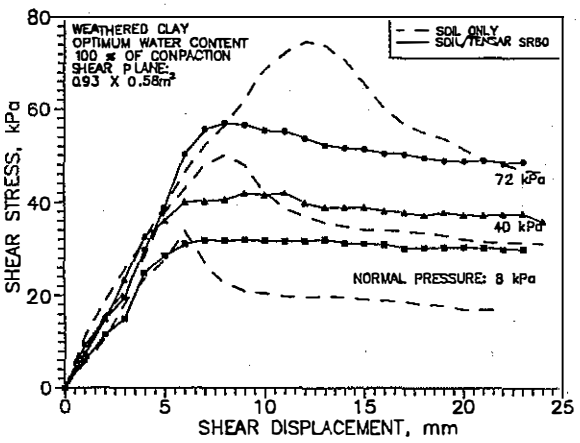


Fig. 2 Large scale direct shear tests for weathered clay/Tensar SR80 interface

the top cover of the pullout box. The large scale direct shear apparatus was developed on the same frame as the pullout box with additional upper shear box and reaction frame. The shear area is 0.54 m$^2$ (0.93 m by 0.58 m). The shear force was applied by the same pullout jack through four 12.7 mm in diameter steel bars which were welded infront of the upper box just above the predetermined shear surface and the normal pressure was also applied by pressurized air bag.

The pullout or direct shear force was measured by a load cell attached between the reinforcement and the pullout jack. The displacement was monitored by Linear Variable Differential Transformer (LVDT) supplemented by dial gauges. Strain gauges were used to measure the strains developed in the transverse and longitudinal members of the reinforcement during the pullout test. The displacements along the extensible reinforcements during the pullout tests were measured by using the inextensible piano wire-dial gauge displacement measuring system.

The multistage test procedure was adopted for large scale direct shear and pullout of steel grid reinforcements. First, the test was done at certain applied normal pressure. When the desired displacement was reached, the normal pressure was increased for subsequent test. Using this method, in one set up, three tests can be done. The tests are categorized as first stage tests, second stage tests, and third stage tests. For Tensar grids, pullout tests were continued until the grid was broken. The shear or pullout rate of 1 mm/min was adopted throughout the test. The normal pressure was varied from 10 to 130 kPa.

## 3 DIRECT SHEAR RESISTANCE

Generally , the direct shear resistance between grid reinforcement and the soil has three components: (a) the shear resistance between the soil and the reinforcement plane surface area; (b) the soil to soil shear resistance at the grid opening; (c) the resistance from soil bearing on reinforcement apertures (Jewell et al 1984). Since the last part is difficult to assess, usually, the influence of the reinforcement apertures on direct shear resistance is treated as to increase the skin friction resistance between the soil and the reinforcement plane surface. Therefore, the direct shear resistance can be expressed in terms of the two contributions from shear between soil and plane surface area of reinforcement and shear between soil and soil.

The commonly used grid reinforcements are steel grids and Tensar grids. Since the steel grids normally have a large opening, and the contact area between the soil and the grid surface is very small, in the case of direct shear mode, the interface is not a weak surface. The interface direct shear tests were only conducted between the soil and Tensar grids.

Figure 2 shows the shear stress/shear displacement curves for the soil/Tensar grid SR80 interface. The shear stress/shear displacement curves using soil specimen only has been combined in the figures as dashed line for comparison. It can be seen that the initial shear modulus between the soil/SR80 interface is nearly the same as that of the soil only. The peak strength of the soil/Tensar grid interfaces is smaller than that of soil only. However, the residual strength is higher than that of the soil only under applied normal pressure of 8 kPa and 40 kPa. Under 72 kPa applied normal pressure, both the soil and the soil/Tensar grid interfaces have nearly equal residual strength. For the soil/Tensar SS2 interface, the tendency is the same, except that initial shear modulus between the soil/SS2 is smaller than that of soil only. It is possible that the soil and SS2 interface has larger portion of resistance from bearing resistance of the apertures on the grid than the soil/SR80 interface, which need a larger shear displacement to be mobilized.

During the tests, the shear plane is forced to occur across the surface longitudinal members. The apertures on the grid act as bearing members. Since the friction angle between the soil and Tensar grid plane surface is lower than the soil to soil friction angle, the peak strength between the soil and the grid interfaces is lower than that of soil only. While for residual strength, in the case of cohesive-frictional soil, the

cohesion resistance reduced quickly when the shear displacement increase, but for soil/Tensar grid interfaces, due to the influence of the apertures on the grids, the strength reduction is less than the soil specimen only. Especially, in the case of very low applied normal pressure, the contribution of the resistance from grid apertures to the total residual resistance is relatively larger than the case of higher applied normal pressure due to the compaction induced residual lateral stress.

In large scale direct shear test, the displacement necessary to mobilize the peak stress for soil and soil/Tensar grid interfaces is varied from 6 mm to 11 mm. The strength parameters were obtained by using Mohr-Coulomb failure law. The friction angle ($\phi_g$) between the soil and the grid surface was obtained by using following equation:

$$\tan\phi_{sg} = \alpha_g \cdot \tan\phi_g + (1-\alpha_g) \cdot \tan\phi \quad ....(1)$$

where $\phi_{sg}$ is friction angle between soil and grid reinforcement, $\phi_g$ is friction angle between soil and grid surface, $\phi$ is friction angle of soil, and $\alpha_g$ is fraction of grid surface area. All parameters are listed in Table 2. It shows that in the test stress levels, the grid apertures influence the strength of adhesion part more than that of friction part. The skin friction angle between the soil and Tensar grids have been found in the range from 6° to 8.5°. At peak strength condition, for the soil/SS2 interface, the skin friction angle of 24.8° was obtained. However, the influence of the grid apertures on skin friction angle is not considered in the Eq. 1. The value may not represent the skin friction angle.

Although the large scale direct shear test results from this study showed that the shear stress/shear displacement relationship is close to a linear elastic-perfect plastic model, it is believed that the large scale direct shear test is suitable for determining the design parameter, but not for studying the constitutive law. Comparing the conventional and large scale direct shear test results for the soil without reinforcement, it was shown that the conventional direct shear tests yielded a nonlinear shear stress/shear displacement curve, while, the large scale direct shear tests gave a nearly linear relationship. Therefore, the hyperbolic model of Clough & Duncan (1971) is suggested to represent the soil/grid reinforcement direct shear interaction mode.

The large scale direct shear test underestimates the shear strength and shear stiffness. The shear force was applied to the soil sample through the back wall of the shear box, due to the compressibility of the soil inside the shear box, the shear strength on shear plane in large scale direct shear test may be mobilized progressively. The overall effect of this progressive strength mobilization process is to reduce the average shear modulus and shear strength of the soil, especially, the cohesion component. Nevertheless, the large scale test results provided reliable shear strength and deformation ratio between the soil and the soil/grid interface. Based on the test results, it is recommended that for cohesive-frictional soil and Tensar grid interfaces, 75% of the soil strength can be used as the interface strength. For initial shear stiffness, it can be taken the same as that of soil only for soil/SR80 interface and 70% of the value of soil for soil/SS2 interface.

**Table 2. Strength parameters from direct shear tests**

| Shear plane | | Cohesion, C, (kPa) | | Friction angle, $\phi$ or $\delta$, (°) | |
|---|---|---|---|---|---|
| | | Peak | Residual | Peak | Residual |
| Soil only | Conventional | 139.5 | | 31.5 | |
| | Large scale | 27.5 | 12.7 | 31.0 | 24.3 |
| Soil/SR80 | Grid | 28.3 | 26.8 | 19.8 | 15.5 |
| | Skin Friction | | | 6.8 | 5.9 |
| Soil/SS2 | Grid | 23.1 | 20.3 | 29.7 | 21.0 |
| | Skin Friction | | | 24.8 | 8.2 |

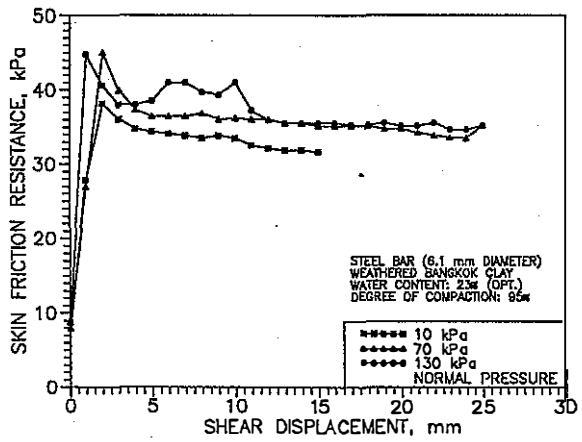


Fig. 3 Skin friction vs. shear displacement between steel bar and weathered clay

## 4 PULLOUT RESISTANCE

The resistance for pullout of grid reinforcement from the soil consists of two parts, namely: friction resistance from soil shearing on grid shearing surface, and passive bearing resistance from soil bearing on grid bearing area which are normal to the direction of relative movement between the soil and the reinforcement. Over 90% of the pullout resistance of steel grid reinforcement is from passive bearing resistance (Chang et al 1977; Palmeira & Milligan 1989). The friction resistance is mobilized earlier than the bearing resistance. The mobilization of resistance of soil bearing on the grid transverse member is caused by the development of soil strain. Therefore, for stiff

**Table 3. Friction resistance between weathered Bangkok clay and steel bar**

| Soil type | Parameters | Weathered clay |
|---|---|---|
| Wet side of optimum | W, (%) | 28.0 |
| | $C_a$, (kPa) | 10.5 |
| | δ,(°) | 4.8 |
| | $d_{cr}$, (mm) | 1-2 |
| Optimum | W, (%) | 23.0 |
| | $C_a$, (kPa) | 30.0 |
| | δ, (°) | 5.0 |
| | $d_{cr}$, (mm) | 1-3 |
| Dry side of optimum | W, (%) | 16.0 |
| | $C_a$, (kPa) | 30.0 |
| | δ, (°) | 10.0 |
| | $d_{cr}$, (mm) | 1-2 |

W : water content.
$C_a$ : adhesion.
δ : skin friction angle.
$d_{cr}$ : displacement for mobilizing the peak friction resistance.

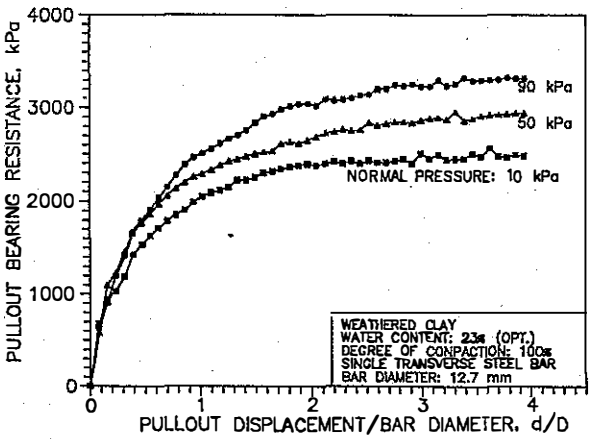


Fig. 4 Typical normalized pullout bearing resistance curves

reinforcement, it depends, to a large extend, on the stress/deformation behavior of the soil.

### 4.1 Pullout Friction Resistance

The pullout friction resistance of steel grid is from the skin friction between the grid longitudinal bars and the backfill soil. The pullout test of the steel bar from the cohesive-frictional soil were conducted by Shivashankar (1991) for studying the maximum skin friction resistance. The results of skin friction between weathered Bangkok clay and steel bar were reanalyzed to study the skin friction mobilization process. Figure 3 is a typical skin friction resistance versus displacement curves for W4.5 (diameter of 6.1 mm) bar embedded in weathered clay which was compacted to 95 degree of standard Proctor compaction test at optimum water content of 23 %. It can be seen that the skin friction resistance versus displacement curves more or less show an elasto-perfectly plastic behavior. The displacement for mobilizing the maximum friction resistance ranged from 1 to 3 mm, and for most cases, it was 2 mm. Also, the skin friction did not increase very much with the increase of applied normal pressure. This means that the skin friction angle is small. The skin friction angle, adhesion, and the displacement for mobilizing the maximum friction resistance together with corresponding compaction water contents are listed in Table 3.

### 4.2 Pullout Passive Bearing Resistance

The pullout tests with single transverse steel bar and steel grid with different bearing member space ratios (S/D) have been conducted to investigate the pullout bearing resistance mobilization process. The bearing member space ratio, S/D, is defined as the bearing member spacing, S, divided by the bearing member thickness, D. The friction resistance was subtracted from the total pullout force to obtain pullout bearing resistance. The pullout bearing resistance means the pullout passive bearing resistance force per unit bearing area. The normalized displacement is the pullout displacement divided by grid reinforcement transverse member thickness or diameter. Using the normalized displacement, the pullout bearing resistance mobilization mechanism for different transverse member thickness can be compared. Figure 4 is a typical normalized pullout bearing resistance curve for isolated single bearing member. The pullout bearing resistance curve for steel grid reinforcement is similar in shape to that in Fig. 4. The shape of the pullout bearing resistance curve indicates that the pullout bearing resistance (stress), $\sigma_b$, normalized displacement, $d_n$, relationship for a isolated bearing member can be modelled by a hyperbolic function. The model takes the following form (Chai 1992):

$$\sigma_b = \frac{d_n}{\frac{1}{E_{ip}} + \frac{d_n}{\sigma_{bult}}} \qquad \ldots.(2)$$

where $E_{ip}$ is initial slope of bearing resistance/normalized displacement curve, and $\sigma_{bult}$ is ultimate value of bearing resistance. $E_{ip}$, and $\sigma_{bult}$ are determined by basic soil and reinforcement properties (Chai, 1992). Due the page limitation of this paper, the following discussion contains only the concepts used for deriving the equations to determine the model parameters. The initial slope of the normalized pullout bearing resistance curve, $E_{ip}$, is related to initial slope of triaxial test stress/strain curve of the backfill soil, and bending stiffness of grid bearing member. The ultimate pullout bearing resistance, $\sigma_{bult}$, is related to

maximum pullout bearing resistance by failure ratio, $R_{fp}$. Limited data showed that the failure ratio of pullout testis approximately the same as of the triaxial test value of the backfill soil. The maximum pullout bearing resistance is influenced by several factors. However, it is mainly controlled by the strength of the backfill soil and the grid bearing member spacing ratio, S/D. Generally, the larger the spacing ratio, the higher the pullout passive bearing resistance from one bearing member or the less interference between bearing members. The maximum pullout bearing resistance of grid reinforcement is determined by multiplying the maximum bearing resistance of a single isolated bearing member with a bearing member spacing ratio influence factor. The maximum pullout bearing resistance of a isolated single bearing member is calculated by bearing capacity theory, based on the characteristic field as shown in Fig. 5. The bearing member interaction is considered by an empirical equation using basic backfill soil and reinforcement properties.

When the applied normal pressure is less than the maximum compaction induced effective stress, and the bearing member space ratio is less than 30, the pullout softening behavior is likely to occur. The softening behavior occur mainly because of the strength reduction in the backfill soil during the pullout process. When considering the pullout softening behavior, the proposed hyperbolic model still can be used to simulate the pullout bearing resistance curve. In this case, it is assumed that the backfill soil strength parameters is reduced from peak value to critical state value when the pullout displacement increased from $d_1$ to $d_2$. Here $d_1$ is related to the bearing member spacing ratio and the displacement necessary to mobilize the peak strength in conventional direct shear tests and $d_2$ is assumed to be five times of $d_1$.

An analytical method of determining the grid reinforcement pullout force/pullout displacement relationship has been established based on the proposed hyperbolic bearing resistance model, elastic-perfectly plastic skin friction relationship, and load transfer mechanism of axially loaded pile (Reese 1964) to consider the extensibility of the grid longitudinal member. Figures 6 and 7 are the comparison of laboratory pullout test results with calculated values for steel grid and Tensar SR80, respectively. It can be seen that the proposed method predicts the pullout curves reasonably well for both inextensible steel grid and extensible Tensar grid reinforcements. The method is very useful for reinforced earth design by checking the necessary embedment length of grid reinforcement to provide required pullout resistance or the displacement to mobilize the desired pullout resistance.

### 4.3 Pullout Bond Coefficient

The item of pullout bond coefficient is the measure of the pullout resistance, which is defined as follows:

$$f_b = \frac{P_n}{2 \cdot L \cdot W \cdot (C + \sigma_n \cdot \tan\phi)} \qquad \ldots(3)$$

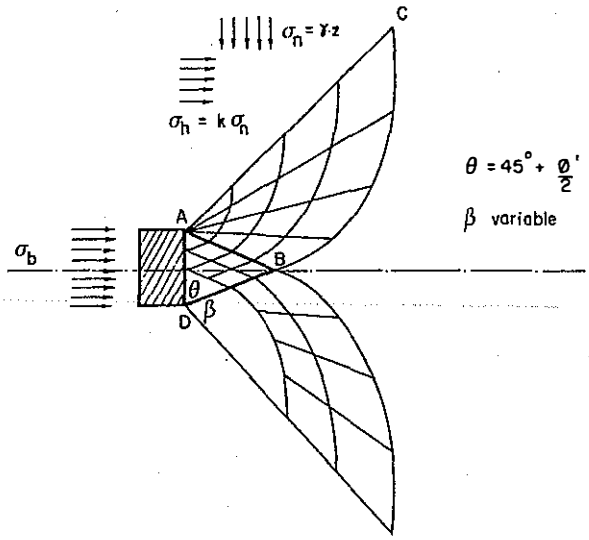


Fig. 5 Proposed stress characteristic field for pullout bearing failure mechanism

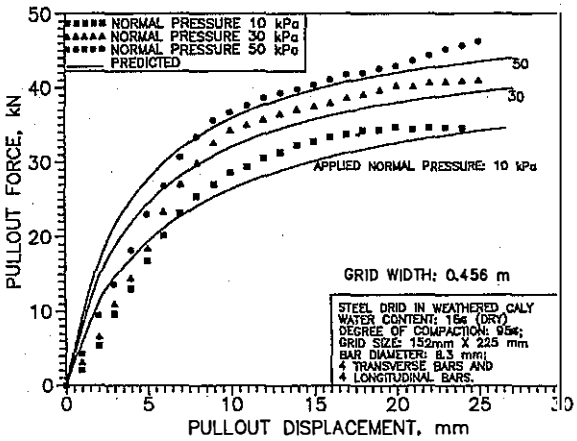


Fig. 6 Comparison of pullout force/pullout displacement curves for steel grid

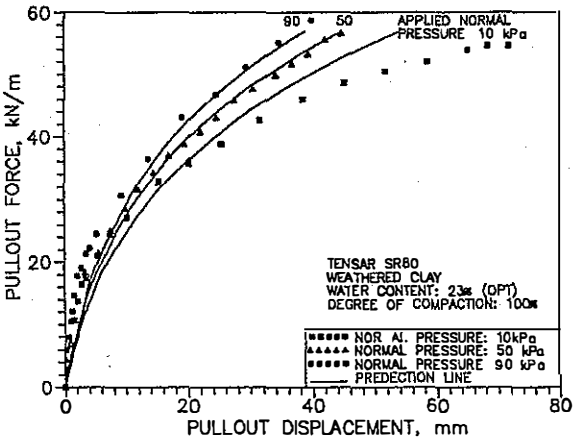


Fig. 7 Comparison of pullout force/pullout displacement curves for Tensar SR80

in which $f_b$ is pullout bond coefficient, $P_n$ is total pullout resistance of grid reinforcement, L and W are length and width of reinforcement providing bond, respectively, C is cohesion of backfill soil, $\phi$ is friction angle of backfill soil, and $\sigma_n$ is the normal pressure.

Pullout test results of steel grids in weathered Bangkok clay showed that for bearing member spacing ratio, S/D, from 8 to 50, the bond coefficient is less than one. This coefficient was about 0.45 for S/D of 8, and 0.2 for S/D larger than 50. The strength parameter of compacted weathered Bangkok clay based on total stresses were C of 120 kPa and $\phi$ of 30.5 degrees.

## 5 CONCLUSIONS

1. The direct shear resistance between soil and grid reinforcement has two contributions from shear resistance between soil and grid reinforcement plane surface and shear resistance between soil and soil. For Tensar geogrids, the test results showed that the soil/Tensar geogrid interfaces yield lower peak strength but higher residual strength than that of the soil to soil due to the mutual effects of smooth plane surface area and the apertures on the grids. It is suggested that the shear stress/shear displacement relationship can be modelled by hyperbolic model of Clough & Duncan (1971).

2. The pullout resistance of grid reinforcements consists of two parts, namely: friction resistance and passive resistance. The friction component is relatively small and needs a small relative displacement to be mobilized. The friction resistance/relative displacement relationship can be simulated by linear elastic-perfectly plastic model. The normalized pullout bearing resistance curve can be modelled by using a hyperbolic function based on basic soil and reinforcement properties. The pullout softening behavior is considered by varying the backfill soil strength parameters from peak to critical state value during the increase of the pullout displacement.

3. The proposed analytical method of determining the grid reinforcement pullout force/pullout displacement relationship provides a useful tool for reinforced earth design. Comparing the calculated and the laboratory pullout test results, the proposed method predicts the pullout curves for both inextensible (steel grids) and extensible (Tensar geogrids) reinforcements reasonably well.

4. For grid reinforcements in cohesive-frictional backfill such as weathered Bangkok clay, the pullout bond coefficient is less than 1.0.

## REFERENCES


Bergado, D.T., Hardiyatimo, H.C., Cisneros, C.B. Chai, J.C., Alfaro, M.C, Balasubramaniam, A.S. & Anderson, L.A. 1992. Pullout resistance of steel geogrids with weathered clay as backfill material. Geotechnical Testing J., Vol. 15, No. 1, 33-46.

Chai, J.C. 1992. Interaction between grid reinforcement and cohesive-frictional soil and performance of reinforced wall/embankment on soft ground. D. Eng. Dissertation, Asian Institute of Technology, Bangkok, Thailand.

Clough, G.W. & Duncan, J.M. 1971. Finite element analysis of retaining wall behavior, J. of Soil Mech. and Found. Eng. Div., ASCE, Vol. 97, No.SM12, 1657-1673.

Janbu, N. 1963. Soil compressibility as determined by oedometer and triaxial tests. Proc. Europ. Conf. Soil Mech. Found. Eng., Wiesbaden, Vol. 1, 19-25.

Jewell, R.A., Milligan, G.W.E., Sarsby, R.W. & Dubois, D. 1984. Interaction between soil and geogrids. Proc. of the Symp. on Polymer Grid Reinforcement in Civil Eng., Thomas Telford Limited, London, U.K., 19-29.

Palmeira, E.M. & Milligan, G.W.E. 1989. Scale and other factors affecting the results of pullout tests of grids buried in sand, Geotechnique, Vol. 39, No.3, pp.511-524.

Peterson, L.M. & Anderson, L.R. 1980. Pullout resistance of welded wire mats embedded in soil, Research Report Submitted to Hilfiker Co., from the Civil and Envir. Eng. Dept., Utah State Univ., Utah, U.S.A.

Reese, L.C. 1964. Load versus settlement for an axially loaded pile, Proc. of the Symp. on Bearing Capacity of Piles, Part 2, Central Bldg Research Inst., Roorkee, India, Cement and Concrete, New Delhi, India, 18-38.

Shivashankar, R. 1991. Behavior of a mechanically stabilized earth (MSE) embankment with poor quality backfills on soft clay deposits, including a study of the pullout resistances, D.Eng. Dissertation, Asian Institute of Technology, Bangkok, Thailand.